Electronic Supplementary Material (ESI) for Nanoscale.

Supporting Information for

High performance Tin Diselenide photodetectors dependent on thickness: Vertical graphene sandwiched device and interfacial mechanism

Wei Gao[1], Zhaoqiang Zheng[1*], Yongtao Li[1], Yu Zhao[1], Liang Xu[3], Huixiong Deng[2*], Jingbo Li[1,2*]

[1] School of Materials and Energy, Guangdong University of Technology, Guangzhou 510006, P. R. China.

[2] State Key Laboratory of Superlattices and Microstructures, Institute of Semiconductors, Chinese Academy of Sciences, Beijing 100083, P. R. China.

[3] Zhejiang Bright Semiconductor Technology Co. Ltd., Jinhua, Zhejiang, 321000, P. R. China.

[*] Corresponding authors: zhengzhq5@mail2.sysu.edu.cn; hxdeng@semi.ac.cn; and jbli@semi.ac.cn

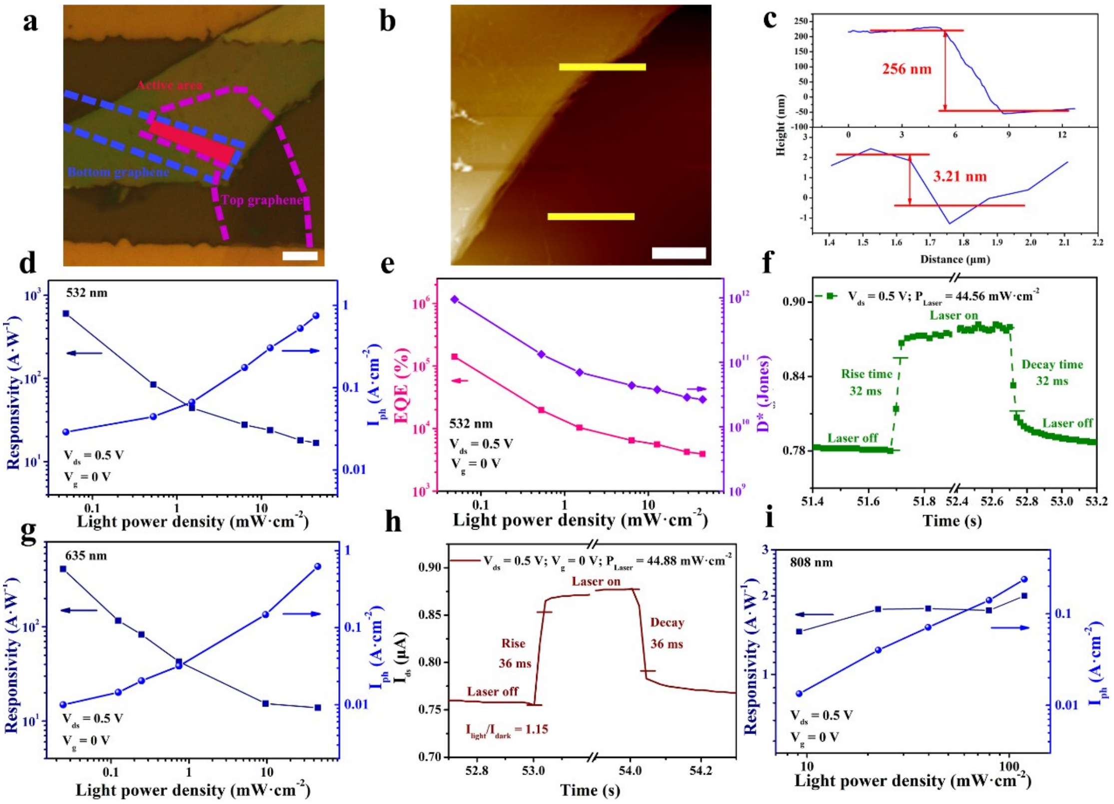

Fig. S1 Optoelectrical characteristics of the Gr-$SnSe_2$ (256 nm)-Gr heterostructure. (a) Optical image of the heterostructure. The scale bar is 5 μm. (b) Atomic Force microscopy (AFM) topography at the interface of the top graphene and $SnSe_2$. (c) The corresponding thickness of the $SnSe_2$ and top graphene from (d) Responsivity and photocurrent density by 532 nm laser as a function of light power density under V_{ds} = 0.5 V, V_g = 0V. (e) EQE and Detectivity as a function of light power density. (f) Rising and decay time of the Gr-$SnSe_2$-Gr under a 532 nm illumination at V_g = 0 V. (g) Responsivity and photocurrent density by 635 nm laser as a function of light power density under V_{ds} = 0.5 V, V_g = 0V. (h) Rising and decay time of the Gr-$SnSe_2$-Gr under a 635 nm illumination at V_g = 0 V. (i) Responsivity and photocurrent density by 808 nm laser as a function of light power density under V_{ds} = 0.5 V, V_g = 0V.

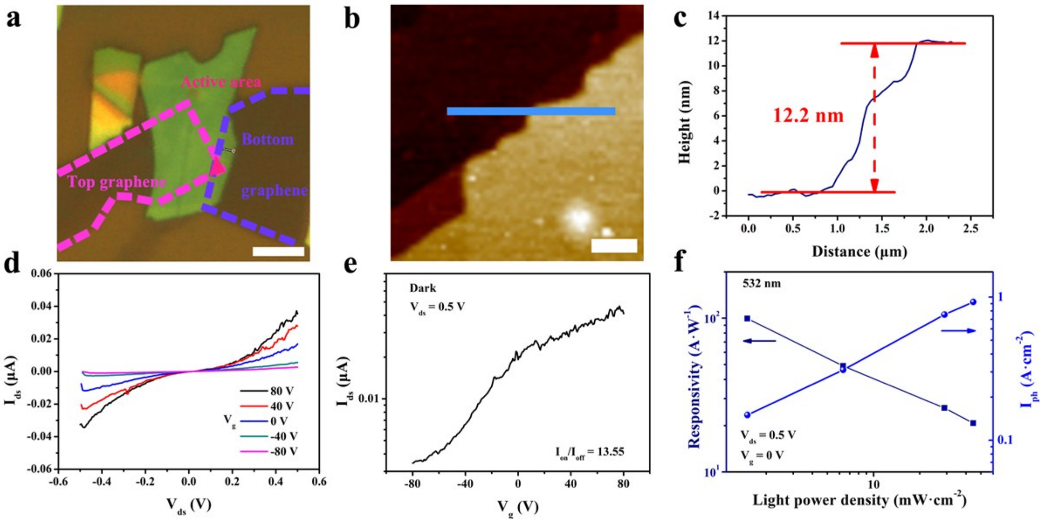

Fig. S2 (Opto) electrical characteristics of the vertical Gr-$SnSe_2$ (12.2 nm)-Gr heterostructure. (a) Optical image of the heterostructure. The scale bar is 5 μm. (b) Atomic Force microscopy (AFM) topography at the interface of $SnSe_2$. (c) The corresponding thickness of $SnSe_2$ from (d) Output characteristic curves of the device under V_g from 80 V to -80 V. (e) Transfer characteristic curves of the device correlated to V_g. (f) Responsivity by 532 nm laser as a function of light power density under V_{ds} = 0.5 V, V_g = 0V.

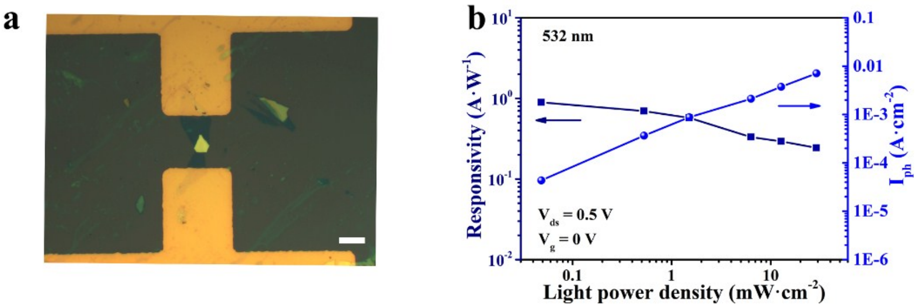

Fig. S3 **(**Opto) electrical characteristics of the vertical Gr-$SnSe_2$ (30.1 nm)-Gr heterostructure. (a) Optical image of the heterostructure. The scale bar is 10 μm. (b) Responsivity by 532 nm laser as a function of light power density under $V_{ds} = 0.5$ V, $V_g = 0$V.

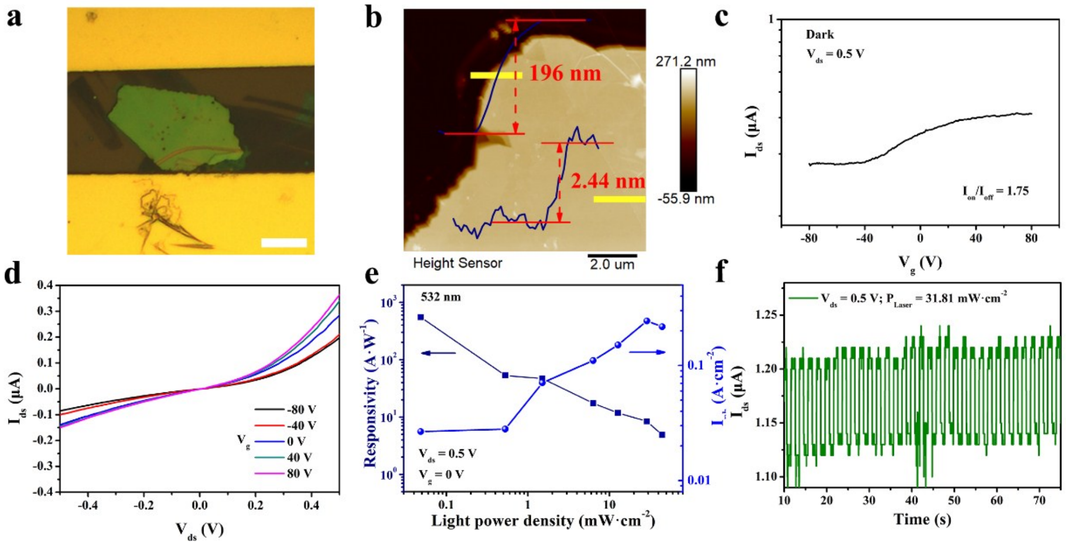

Fig. S4 (Opto) electrical characteristics of the vertical Gr-$SnSe_2$ (196 nm)-Gr device. (a) Optical image of the heterostructure. The scale bar is 10 μm. (b) Atomic Force microscopy (AFM) topography at the interface of $SnSe_2$ and the corresponding thickness of the $SnSe_2$ along the yellow line. (c) Transfer characteristic curves of the device correlated to V_g. (d) Output characteristic curves of the device under V_g from 80 V to -80 V. (e) Responsivity and photocurrent density by a 532 nm laser as a function of light power density under V_{ds} = 0.5 V, V_g = 0V. (f) Rising and decay time of the device under a 532 nm illumination at V_{ds} = 0.5 V, V_g = 0 V.

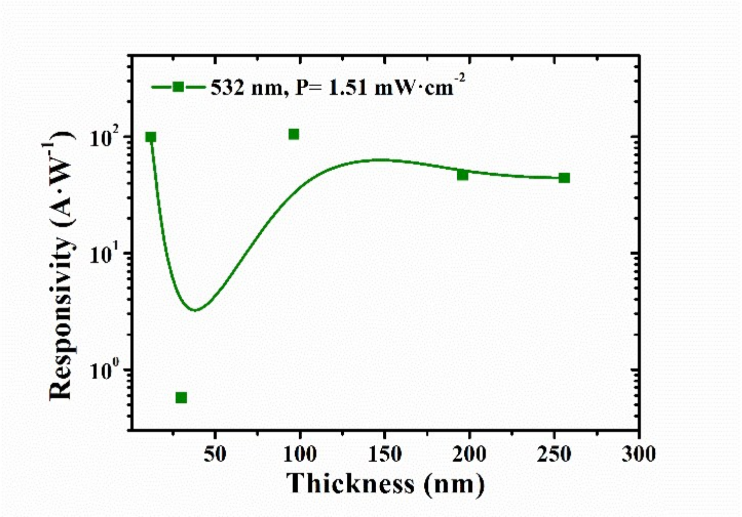

Fig. S5 Thickness-dependent responsivity of $SnSe_2$ nanoflakes.

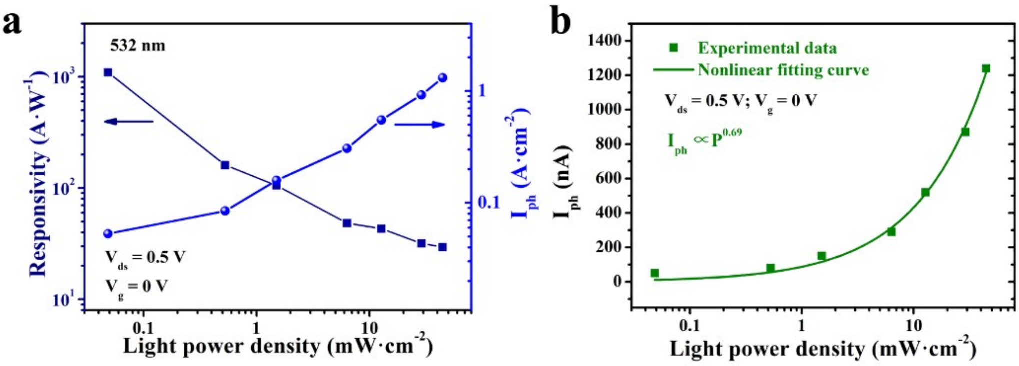

Fig. S6 Optoelectrical characteristics of the Gr-$SnSe_2$ (96.5 nm)-Gr heterostructure. (a) Responsivity and photo-current density as a function of light power density. (b) Light power density dependence of the photocurrent.

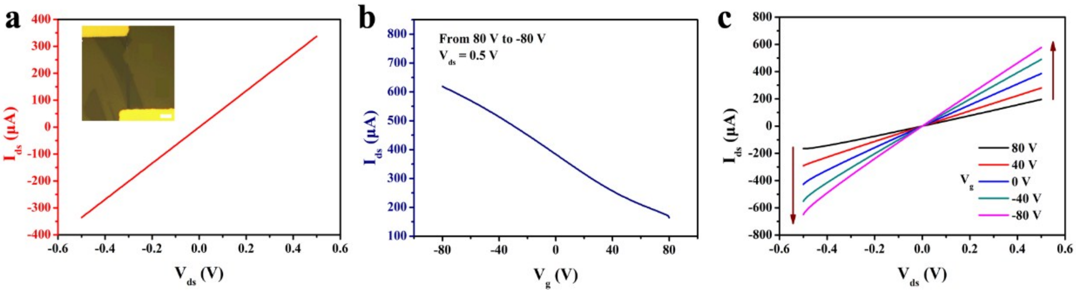

Fig. S7 Electrical properties of the FETs devices for graphene. (a) I_{ds}-V_{ds} characteristic curves without the gate voltage. (b) Transfer curves. (c) Output curves. The scale bar is 10 μm.

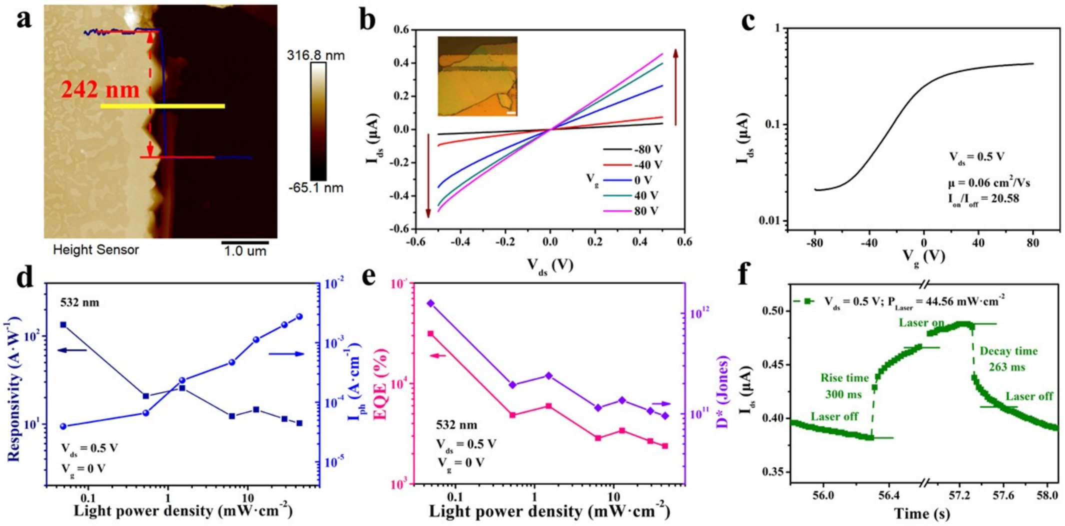

Fig. S8 (Opto) electrical characteristics of the horizontal $SnSe_2$ (242 nm) device. (a) Atomic Force microscopy (AFM) topography at the interface of $SnSe_2$ and the corresponding thickness of the $SnSe_2$ along the yellow line. (b) Output characteristic curves of the device under V_g from 80 V to -80 V. (c) Transfer characteristic curves of the device correlated to V_g. (d) Responsivity and photocurrent density by a 532 nm laser as a function of light power density under V_{ds} = 0.5 V, V_g = 0V. (e) EQE and Detectivity as a function of light power density. (f) Rising and decay time of the device under a 532 nm illumination at V_{ds} = 0.5 V, V_g = 0 V.

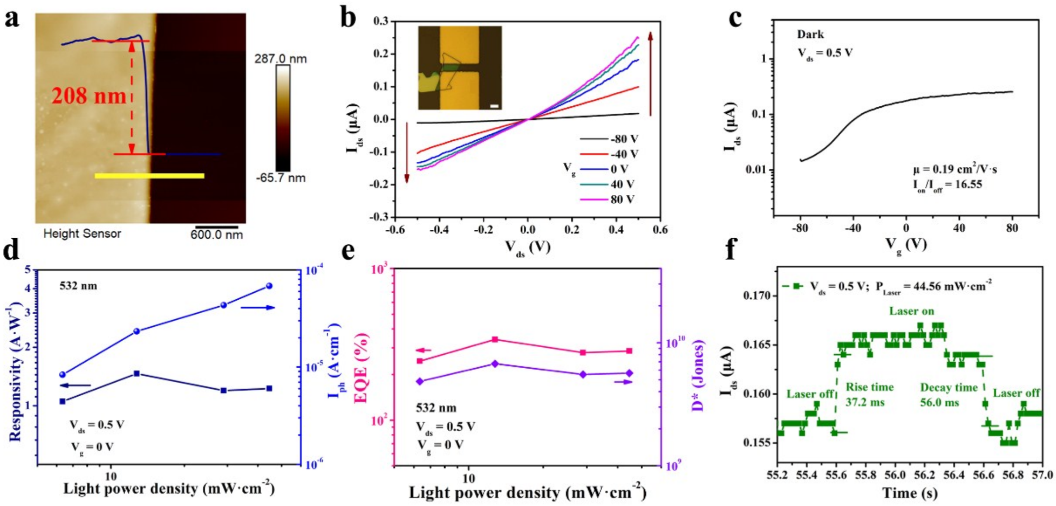

Fig. S9 (Opto) electrical characteristics of the horizontal $SnSe_2$ (208 nm) device. (a) Atomic Force microscopy (AFM) topography at the interface of $SnSe_2$ and the corresponding thickness of the $SnSe_2$ along the yellow line. (b) Output characteristic curves of the device under V_g from -80 V to 80 V. (c) Transfer characteristic curves of the device correlated to V_g. (d) Responsivity and photocurrent density by a 532 nm laser as a function of light power density under V_{ds} = 0.5 V, V_g = 0V. (e) EQE and Detectivity as a function of light power density. (f) Rising and decay time of the device under a 532 nm illumination at V_{ds} = 0.5 V, V_g = 0 V.

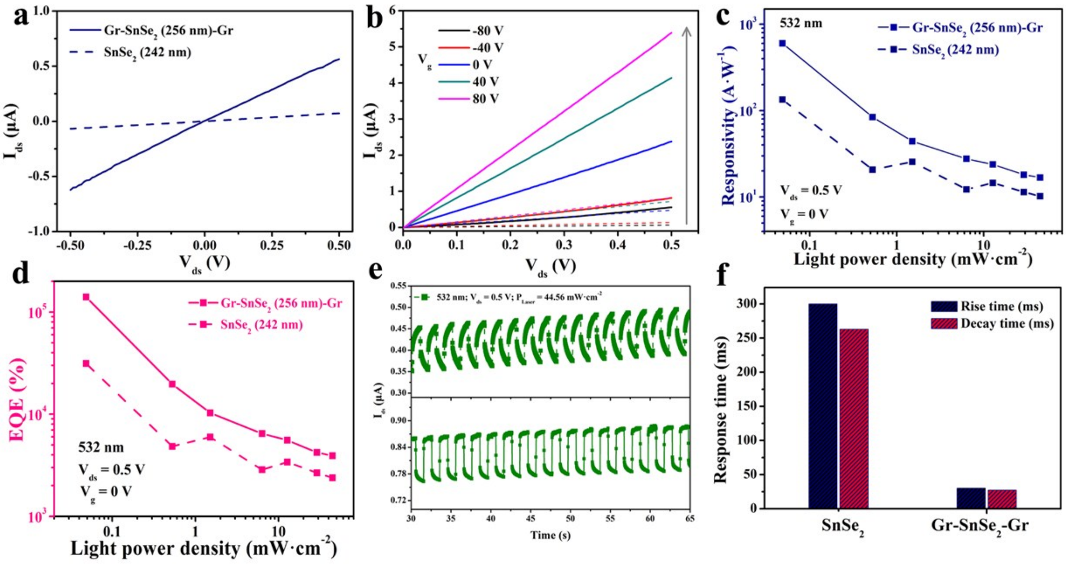

Fig. S10 (Opto) electrical characteristics of the Gr-SnSe$_2$ (256 nm)-Gr compared to the horizontal SnSe$_2$ (242nm) device under V_{ds} = 0.5 V, V_g = 0 V. (a) I_{ds}-V_{ds} curve of the device. (b) Output characteristic curves of the device under V_g from -80 V to 80 V. (c) Responsivity by 532 nm laser as a function of light power density. (d) EQE and Detectivity as a function of light power density. (e) Time trace of SnSe$_2$ (top) and Gr-SnSe$_2$-Gr (bottom) under a 532 nm illumination. (f) Rising and decay time of the device under a 532 nm illumination.

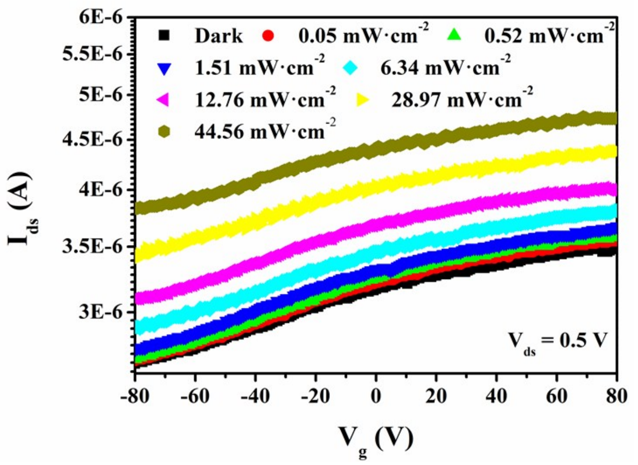

Fig. S11 The I_{ds}-V_g curves under 532 nm illumination as a function of light power density.

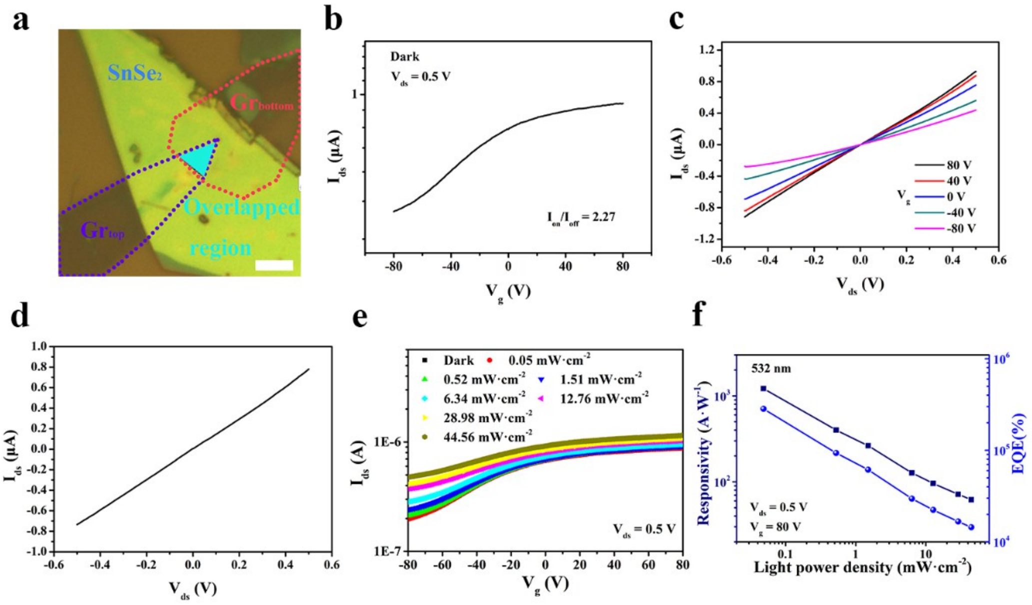

Fig. S12 (Opto) electrical characteristics of the vertical Gr-$SnSe_2$(~100 nm)-Gr device. (a) Optical image of the heterostructure. The scale bar is 5 μm. (b) Transfer characteristic curves of the device correlated to V_g. (c) Output characteristic curves of the device under V_g from 80 V to -80 V. (d) I_{ds}-V_{ds} curve under dark condition. (e) The I_{ds}-V_g curves under 532 nm illumination as a function of light power density. (f) Responsivity and photo-current density as a function of light power density.

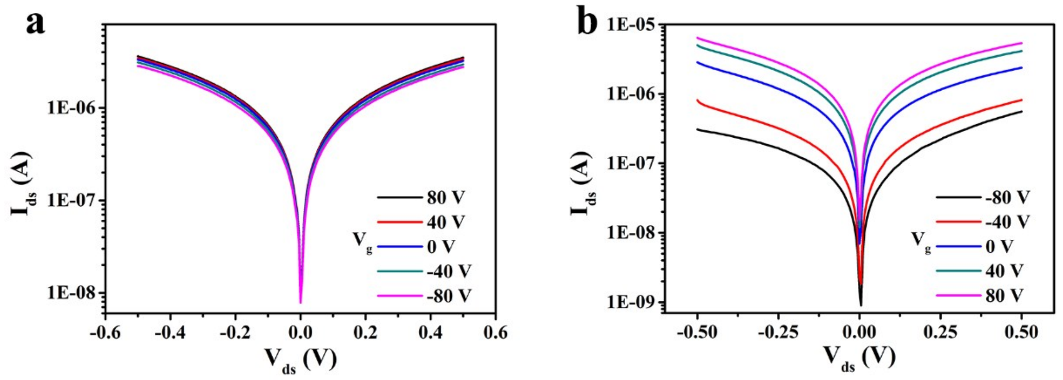

Fig. S13 Electrical properties of the Vertical Gr-$SnSe_2$-Gr devices dependent on different thickness: Logarithmic output characteristic curves of the device under V_g from 80 V to -80 V. (a) 96.5 nm. (b) 256 nm.

Table S1 Comparison of figures-of-merit for vertical graphene-photodetectors based on 2D layered materials

Materials	Measurement condition	Responsivity (A/W)	EQE (%)	D* (Jones)	Response time	Ref.
Graphene-thick $SnSe_2$-Graphene	532 nm $V_g = 80$ V $V_{ds} = 0.5$ V	1.3×10^3	3×10^5	1.2×10^{12}	38.2 ms /32 ms	This work
Graphene-$MoTe_2$ -Graphene	1064 nm $V_g = 30$ V $V_{ds} = 0$ V	0.11	12.9	/	24 μs	1
Graphene-n-InSe -Graphene	633 nm $V_g = 0$ V $V_{ds} = 2$ V	10^5	10^5	10^{13}	/	2
Graphene-MoS_2 -Graphene	514 nm $V_g = -60$ V $V_{ds} = 0.5$ V	/	25	/	50 μs	3
Graphene-p-GaSe/ n-InSe-Graphene	410 nm $V_g = 0$ V $V_{ds} = 2$ V	350	/	3.7×10^{12}	2 μs	4
Graphene-Ta_2O_5 -Graphene	532 nm $V_{ds} = 1$ V	10^3	/	/	0.75 s	5

Graphene-WSe$_2$/GaSe-Graphene	520 nm $V_g = 0$ V $V_{ds} = -1.5$ V	6.2±0.2	1490±50	/	30 μs	6
Graphene-GaSe/WS$_2$-Graphene	410 nm $V_g = 0$ V $V_{ds} = 2$ V	149	/	4.3×10^{12}	37 μs/43 μs	7
Graphene-WSe$_2$-Graphene	759 nm $V_g = 0$ V $V_{ds} = 0.5$ V	/	7.3	/	1.6 ns	8
h-BN-Graphene-MoS$_2$/WSe$_2$-Graphene	532 nm $V_g = 0$ V $V_{ds} = 0$ V	0.12	34	/	/	9

References

1. K. Zhang, X. Fang, Y. Wang, Y. Wan, Q. Song, W. Zhai and L. Dai, *ACS Appl. Mater. Inter.*, 2017, 9, 5392-5398.
2. G. W. Mudd, S. A. Svatek, L. Hague, O. Makarovsky, Z. R. Kudrynskyi, C. J. Mellor and E. E. Vdovin, *Adv. Mater.*, 2015, 27, 3760-3766.
3. W. J. Yu, Y. Liu, H. Zhou, A. Yin, Z. Li, Y. Huang and X. Duan, *Nat. Nanotechnol.*, 2013, 8, 952-958.
4. F. Yan, L. Zhao, A. Patanè, P. Hu, X. Wei, W. Luo and K. Chang, *Nanotechnology*, 2017, 28, 27LT01.
5. C. Liu, Y. Chang, T. B. Norris and Z. Zhong, *Nat. Nanotechnol.*, 2014, 9, 273-278.
6. X. Wei, F. Yan, Q. Lv, C. Shen and K. Wang, *Nanoscale*, 2017, 9, 8388-8392.
7. Q. Lv, F. Yan, X. Wei and K. Wang, *Adv. Opt. Mater.*, 2018, 6. 1700490.
8. M. Massicotte, P. Schmidt, F. Vialla, K. G. Schädler, A. Reserbat-Plantey, K. Watanabe, T. Taniguchi, K. J. Tielrooij and F. H. Koppens, *Nat. Nanotechnol.*, 2016, 11, 42-46.

9. C. H. Lee, G. H. Lee, A. M. Van Der Zande, W. Chen, Y. Li, M. Han, X. Cui, G. Arefe, C. Nuckolls, T. F. Heinz, J. Guo, J. Hone and P. Kim, *Nat. Nanotechnol.*, 2014, 9, 676-681.